Environ Geol (2006) 50: 941–961
DOI 10.1007/s00254-006-0264-7

ORIGINAL ARTICLE

Aldo Clerici
Susanna Perego
Claudio Tellini
Paolo Vescovi

A GIS-based automated procedure for landslide susceptibility mapping by the Conditional Analysis method: the Baganza valley case study (Italian Northern Apennines)

Received: 22 November 2005
Accepted: 9 March 2006
Published online: 4 April 2006

A. Clerici (✉) · S. Perego · C. Tellini
P. Vescovi
Dipartimento di Scienze della Terra,
Universitá degli Studi di Parma,
43100 Parma, Italy
E-mail: aldo.clerici@unipr.it
Fax: +39-0521-905305

Abstract Among the many GIS based multivariate statistical methods for landslide susceptibility zonation, the so called "Conditional Analysis method" holds a special place for its conceptual simplicity. In fact, in this method landslide susceptibility is simply expressed as landslide density in correspondence with different combinations of instability-factor classes. To overcome the operational complexity connected to the long, tedious and error prone sequence of commands required by the procedure, a shell script mainly based on the GRASS GIS was created. The script, starting from a landslide inventory map and a number of factor maps, automatically carries out the whole procedure resulting in the construction of a map with five landslide susceptibility classes. A validation procedure allows to assess the reliability of the resulting model, while the simple mean deviation of the density values in the factor class combinations, helps to evaluate the goodness of landslide density distribution. The procedure was applied to a relatively small basin (167 km^2) in the Italian Northern Apennines considering three landslide types, namely rotational slides, flows and complex landslides, for a total of 1,137 landslides, and five factors, namely lithology, slope angle and aspect, elevation and slope/bedding relations. The analysis of the resulting 31 different models obtained combining the five factors, confirms the role of lithology, slope angle and slope/bedding relations in influencing slope stability.

Keywords Landslide susceptibility map · Geographic information systems (GIS) · GRASS · Shell script · Northern Italian Apennines

Introduction

The interest of scientists in methodologies assessing the spatial probability of future landslides is testified by the exponentially growing mass of papers proposing methods and applications for landslide susceptibility zonation.

As the methods are too many for a detailed analysis and the related papers too many to be listed, we refer the reader to the papers of Soeters and van Westen (1996), Aleotti and Chowdhury (1999) and Guzzetti et al. (1999) for thorough critical examinations of the different techniques and exhaustive reference lists; here we will provide no more than a schematic classification of the methods, limiting the citations to the most recent papers.

Besides some promising applications of fuzzy logic and artificial neural network, most used methods can be divided into three distinct categories, even if mixed strategies are often adopted: the deterministic (or engineering, or geotechnical), the heuristic (or index) and the statistical methods.

For studies on a regional scale, the heuristic and the bivariate and multivariate statistical methods appear to

be better suited for assessing landsliding probability (Chung et al. 2002;Dai and Lee 2002, 2003; Dai et al. 2002; Donati and Turrini 2002; Lee et al. 2002; Santacana and Corominas 2002; Zhou et al. 2002; Çevik and Topal 2003; Fernandez et al. 2003; Lin and Tung 2003; Ohlmacher and Davis 2003; Remondo et al. 2003; Santacana et al. 2003; van Westen et al. 2003; Ayalew and Yamagishi 2004, 2005; Ayalew et al. 2004; Fernandes et al. 2004; Ko Ko et al. 2004; Lan et al. 2004; Lee 2004; Lee and Choi 2004; Perotto-Baldiviezo et al. 2004; Raghavan et al. 2004; Süzen and Doyuran 2004).

In the heuristic methods, the instability factors are ranked and weighted according to their assumed or expected importance in causing slope failures. As the ranking and weighting rules are based on the experience of geoscientists involved, this approach entails a substantial degree of subjectivity. For this reason, the use of these methods is progressively diminishing, particularly with the diffusion of the GIS technologies, which facilitate more efficient statistical approaches.

The statistical methods are more objective, formally more rigorous and better suited for assessing landsliding probability especially at medium scales. All the statistical methods, despite the methodological and operational differences, are based on the common assumption that slope-failure in the future will be more likely to occur under those conditions which led to past and present instability. In other words, landslide prediction for areas currently free of landslides is carried out by evaluating the similarity between the conditions in such areas and those conditions that have led to landslides in the past. Therefore the conceptual model consists in:

1. the mapping of the landslides,
2. the mapping of a set of factors which are supposed to be directly or indirectly connected with slope instability,
3. the classification of the land surface according to the degree of landslide susceptibility on the basis of the detected statistical relationships between instability factors and instability phenomena.

As each landslide type can originate under different conditions, separate analysis should be performed for different landslide types (Soeter and van Westen 1996; Guzzetti et al. 1999; Remondo et al. 2003). There is a substantial difference between bivariate and multivariate statistical methods. The bivariate methods evaluate the relationship between landslides and each single factor. The misleading aspect of this procedure is that a factor can be seen as irrelevant when considered alone but can result determinant in combination with other variables. In multivariate methods, on the contrary, the relationship between landslides and a number of factors considered simultaneously is evaluated. The most used multivariate techniques are the classical linear and logistic regression and the discriminant analysis.

Although these techniques generally produce satisfactory results, they also require strict assumptions that are frequently violated in practice. Some of them in fact require data derived from a normally distributed population, or similarity in variance–covariance matrices, or assume a linearity in the relationship among variables; others require specific measurement scale for the variables (Carrara et al. 1992). To avoid these obstacles, distributions that differ from normality are often assumed, non-linear relationships among the variables are adopted or transformations of variables from one measurement scale to another are carried out. These operations substantially complicate the process and make the final result difficult to evaluate at least for operators who are not well trained in the field of statistics like landplanners and decision-makers.

Besides the above mentioned classic statistical techniques, there are other less complicated and conceptually straightforward multivariate statistical approaches for producing maps that are easy to comprehend and assess also by non-specialists.

Among them, the so called Conditional Analysis method (Carrara et al. 1995a, b) is conceptually simple and highly compatible with GIS operating features. For these reasons, we decided to adopt this method in a research program aiming to produce Landslide Susceptibility maps, as defined by Brabb (1984), of large areas of the Italian Northern Apennines. As the method requires a long and well defined sequence of operations that makes the procedure tedious and error prone even for well trained GIS users, a shell script, or shell program, mainly based on GIS commands, was created. The script, starting from a Landslide Inventory map and a number of factor maps, automatically carries out the entire procedure up to the construction of the final map portraying the different probabilities of future landslide occurrence. In the following pages, the main characteristics of the current version of the script and its application to the susceptibility zonation of the Baganza torrent basin, in the Emilia sector of the Apennines, are described.

The Conditional Analysis method

In this method, a number of data layers representing factors which are thought to be directly or indirectly connected with landsliding, are overlayed (or crossed, in the jargon of the GIS used in this work) in order to obtain all the possible combinations of the various classes of the different factors. Each of the resulting combinations represents a terrain unit defined as a unique condition unit (UCU) (Carrara et al. 1995a, b),

unique condition subareas (Chung et al. 1995) or unique condition class (Bonham-Carter 1994). Subsequently, the landslide density is computed in each UCU. Assuming the already mentioned principle that slope failures in the future are more likely to occur under those conditions which led to slope failures in the past, the computed landslide density is equivalent to the future landslide probability. Formally, the conditional probability is given by (Carrara et al. 1995a, b):

$$P(L|UCU) = \frac{(\text{landslide area} \cap \text{UCU area})}{\text{UCU area}}, \quad (1)$$

i.e. the conditional probability of landslide occurrence (L) given a unique combination of factors (UCU) is given by the landslide density in that specific UCU.

The final map is constructed by defining a number of density classes and assigning each UCU to the corresponding class according to its computed density. All methods for susceptibility zonation present some problematic aspects mainly regarding the assessment of landslide presence, the choice of the factors to use in the analysis and the evaluation of the reliability of the resulting zonation. Given their importance, these aspects, with the solutions adopted in the proposed procedure, will be discussed in detail in the following sections.

The main scarp upper edge as the landslide representative element

One problem regards the notion of landslide in terms of the assessment of landslide presence and the evaluation of instability factors in correspondence with each landslide. As is very well known, in a landslide two genetically and morphologically distinct zones can be identified: the depletion zone (or detachment zone, or rupture zone), i.e. the upper part of the landslide where the failure is effectively generated, and the accumulation zone, i.e. the lower part which is simply affected by the arrival of the depleted material. Since the susceptibility assessment by statistical methods claim to identify the conditions under which landslides were (and will be) generated, the analysis has to be restricted to the area in which the landslide originated, i.e. the depletion zone, as performed in many works (Chung and Fabbri 1999; Chung et al. 2002; Donati and Turrini 2002; Fernandez et al. 2003; Remondo et al. 2003; Süzen and Doyuran 2004; Ayalew and Yamagishi 2005). In fact, if the whole landslide is considered in assessing the factor combination and in computing the landslide density, the combinations present in the accumulation zone are erroneously considered to be prone to landsliding. However, the depletion zone is generally difficult to identify completely since it is partially occupied by the displaced material. Usually, only the higher portion of this zone, the so called main scarp, and, in particular, its upper edge, is clearly evident due to the slope angle difference with the surrounding unfailed zones: at the contact with the landslide's crown and along the flanks of the depletion zone. So the main scarp upper edge (MSUE) is the most evident morphological feature of a landslide and can easily be identified and mapped both by aerial photographs and on the field.

It must also be considered that all the statistical methods based on the conceptual model expressed above, require knowledge of the factor conditions before the landslide occurrence. With the exception of very recent landslides, the available maps and photographs obviously represent the situation after landsliding. Some factors, such as the bedrock lithology, can be supposed not to have been modified by the landslide occurrence, so the currently observable situation at the depletion zone, or along the MSUE, can be considered to be the same as at time of failure. On the contrary, other features, and in particular morphometric factors like slope angle or aspect, are substantially modified by landsliding. If it is virtually impossible to reliably reconstruct the old topography, it nevertheless seems plausible to assume that the morphometric characteristics which most resemble those present at the failure time are those currently observable in the immediate surroundings of the depletion zone, i.e. along the unmodified external belt of the MSUE. Furthermore, the MSUE has the further advantage of a linear development that is practically independent of how much the material has shifted in the depletion zone, so its length is strictly proportional to the planimetric surface of the depletion zone, at least for the same type of landslide. Therefore the MSUE length provides a reliable measurement of the landslide size.

For all these characteristics the MSUE can be considered to be an easily measurable morphological element which is particularly representative of the genetical part of a landslide and can be profitably used for determining both the instability-factor combination connected to landslide and the landslide dimension.

A similar approach has been adopted by Süzen and Doyuran (2004) who consider a buffer around the crown and flanks of the landslide as the best undisturbed morphological zone representing conditions before landslide occurrence. In the method proposed here, the MSUEs are extracted from the main scarp in the Landslide Inventory raster map, following the procedure illustrated in Fig. 1. Each extracted MSUE is made up of a linear feature with a single cell width.

For each MSUE cell, the class value of each factor is defined. This is performed by a paired analysis of the MSUE map and each single factor map. To each MSUE cell is assigned the factor class value present in a cell of the factor map located at a distance from the MSUE cell ranging from a minimum of 0 to a maximum of 3 cells,

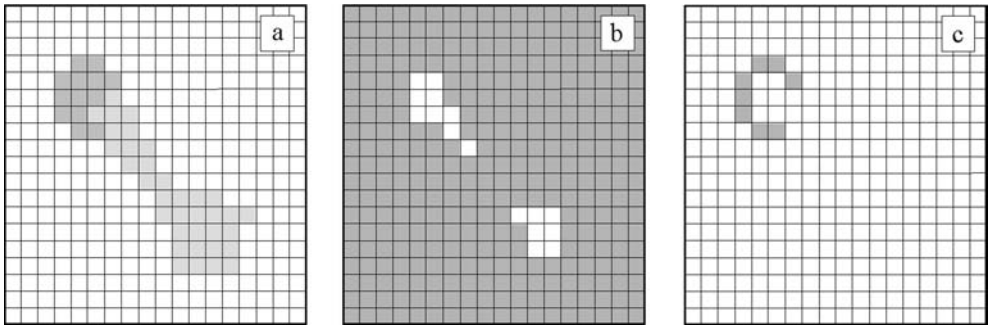

Fig. 1 Process adopted to extract the main scarp upper edge (*MSUE*) from a mapped landslide main scarp. In **a**, a landslide with different category values assigned to the main scarp area (*dark gray*) and to the accumulatione zone (*light gray*) is shown. The area external to landslide is grown by one cell along its margins, producing the effect of adding a cell belt along the inner landslide perimeter, as shown in (**b**). The MSUE is defined by the eight cells common to the main scarp of map (**a**) and to the grown area of map (**b**), as shown in (**c**)

as selected by the user on the basis of the type of factor being considered. If a distance of 0 cell is adopted, the factor values are defined in coincidence with the MSUE. For the factors calculated considering neighboring cells, e.g. slope angle and aspect, it is obviously necessary to adopt a distance greater than 0. This to avoid, or at least to limit, the probability of selecting factor values that were calculated by using some cells on the main scarp or on the accumulation zone. The process is illustrated in Fig. 2 for a single landslide.

At the end of the process, a set of factor values (or landslide factor combination, LFC) is defined for each MSUE cell; according to the basic principle of the Conditional Analysis method the LFC should represent the factor combination present in the cell at the failure time. Having adopted the MSUE to define the landslide dimension and the landslide factor combination, the landslide density for each UCU is obtained by dividing the total length (in meters) of the MSUEs pertaining to each specific LFC by the area (in km^2) of the UCU with the same factor combination as the LFC. The landslide density is therefore expressed in m/km^2 and the above reported landslide probability (1) is modified as follows:

$$P(L|UCU) = \frac{(\text{MSUE length} \cap \text{UCU area})}{\text{UCU area}}. \qquad (2)$$

In the procedure five intervals are defined to classify density values. These intervals are designed in such a way that the mean density value represents the midpoint of the middle class (class 3) and the classes from 1 to 4 have the same interval. The upper limit of the fifth class is open. More precisely, calling Md the mean density, the class interval is Ci = (2/5)Md and the five susceptibility class intervals are: 0–Ci (very low), Ci–2Ci (low), 2Ci–3Ci (medium), 3Ci–4Ci (high), > 4Ci (very high).

In this paper, the landslide mean density was considered a convenient reference value to define the susceptibility of an area and the subdivision in five classes a reasonable compromise between an effective susceptibility differentiation and the readability of the map (Chung et al. 1995; Nagarajan et al. 2000; Çevik and Topal 2003; Ayalew et al. 2004; Perotto-Baldiviezo et al. 2004; Ayalew and Yamagishi 2005). However, this choice hampers the comparison with the susceptibility of other areas having a different mean density, even if obtained following the same procedure.

Factor choice and factor class definition

Theoretically, any geological, geomorphological, climatic and vegetational characteristic, or factor, can be introduced into the analysis, on condition that it can be expressed in some measuring scale (continuous, categorical or nominal), has spatial variability and is defined all over the study area. In practice, as data acquisition may be a very costly and time-consuming operation, the analysis is usually limited to those factors that are known, from previous works on the subject, or at least suspected, to be directly or indirectly connected to landsliding.

A further limitation is connected to the age of formation of the landslides to be analyzed. In fact, as above mentioned, the statistical methods require the knowledge of the conditions at the failure moment. If old landslides are introduced in the analysis, only time-invariant (or quasi-static, long-term, permanent, intrinsic, stationary) conditioning factors, like geological or morphometric characteristics, that may be supposed to change over a geomorphological time scale, can be used in the analysis (Lopez and Zink 1991; Atkinsons and Massari 1998; Binaghi et al. 1998; Guzzetti et al. 1999; Zêzere et al. 1999; Dai and Lee 2002; Zhou et al. 2002; Çevik and Topal 2003). Time-variant (dynamic, extrinsic, or transient) factors, like landuse, human activity or even climatic conditions, that may vary rapidly in response to environmental changes or economical needs, can be used only for recent or very recent landslides. The introduction of post-landslide conditions can completely

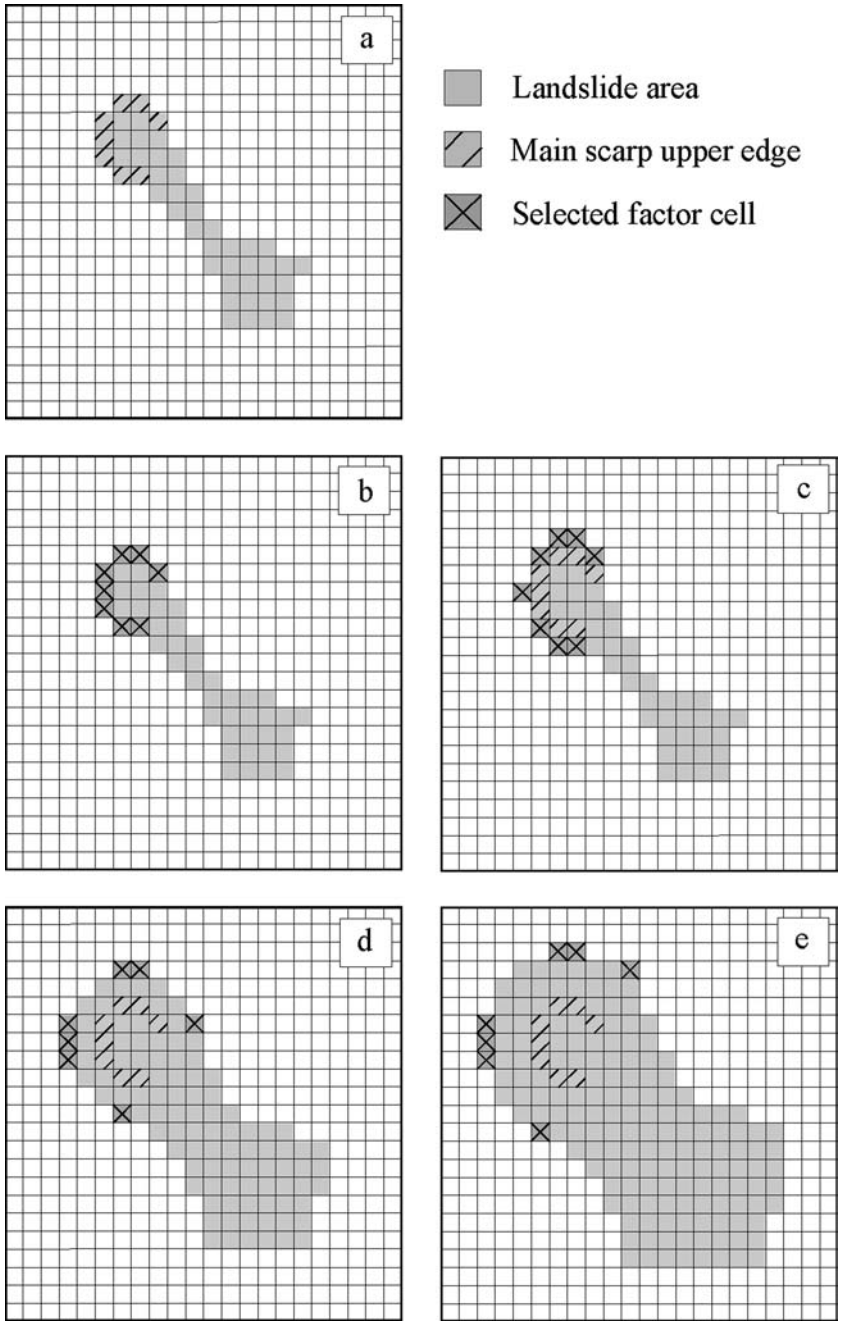

Fig. 2 Factor value definition for the MSUE cells. In **a**, a landslide with the main scarp cells highlighted is shown. If distance of 0 is adopted, the factor values are defined in coincidence with the MSUE cells, as shown in (**b**). For distances greater than 0, a factor cell must be outside the landslide area in order to be selected. In **c**, with a search distance of 1 cell, a 3×3 cell moving matrix centred on the MSUE cells is used and the factor cells are selected along the external belt immediately adjacent to the MSUE. In **d**, with a distance of two cells, the moving matrix has a 5×5 cell size and the landslide area is grown of one cell along the perimeter. In **e**, a 7×7 matrix and a landslide area grown by two cells are used. When a moving matrix is used, like in **c**, **d** and **e**,the factor cell search proceeds clockwise beginning with the vertical and horizontal cells, then along the diagonal ones. Note that in **d** and **e**, the lowest factor cell is selected for both the lowest MSUE cells

reverse the resulting role of a factor, as pointed out by Atkinson and Massari (1998) for reforested areas.

Some problems may also be related to the definition of the factor classes. In the Conditional Analysis method small area classes should be avoided, in order to limit the presence of UCU of small dimensions resulting from the overlay of data layers. Small UCUs have little statistical significance although they can represent rare but physically meaningful conditions. In the case of categorical variables, like for example lithology or landuse, the classes are automatically defined by the original differences of the mapped categories possibly grouped according to some common characteristic.

In the case of continuous variables, as for example slope angle, the subdivision in a convenient number of classes is a user choice and different techniques have been proposed by different authors as described in detail in Süzen and Doyuran (2004). In this work we adopted a subdivision of the factor values in equal interval classes. This method is sufficiently objective and generally pro-

duces classes of similar sizes which are ample enough to be statistically meaningful.

Model validation

Undoubtedly the only rigorous way to evaluate the reliability of a susceptibility map in forecasting landslides, is to wait for future landslides and compare their distribution with the susceptibility classes in the map (Soeters and van Westen 1996; Ermini et al. 2005). However, this "wait and see" method is clearly impractical because many years would probably be required to generate a number of new landslides high enough to allow a meaningful model validation. For this reason, other immediate validation procedures have been proposed by various authors. The most used, and the most similar to the "wait and see" method consists in randomly splitting the past landslides into two distinct sets: the first set is used for the model construction (training, learning, or development set), the second for the model validation (validation, or test set). Conceptually, this second set is assigned the role of future landslides and its distribution in the susceptibility classes constructed using the training set is checked. In Santacana and Corominas (2002), Chung and Fabbri (2003) and Remondo et al. (2003), the basic strategies to obtain two independent sets of landslides are clearly described and a long list of papers dealing with validation procedures is reported.

A similar approach has been introduced in the procedure used here. In the shell script, it is possible to consider two distinct groups of landslides functioning as training and validation sets. A validation table is constructed for each landslide type (see Table. 4, 5, 6, 7 as examples), reporting for each of the five susceptibility classes the percentage of the MSUE length of the training set, the percentage of the MSUE length of the validation set, and the absolute value of their difference. The sum of the percentage differences gives an index, here defined validation error (VE), to evaluate the model as a whole; the smaller the index, the better the model validation, since an higher portion of the MSUE lengths of the validation set has been correctly assigned. The theoretical range of VE is from 0, when all the MSUE percentages of the validation set equal the percentages of the training set, to 200, when all the MSUEs of the validation set are assigned to one or more classes of the training set having 0 value.

For a correct evaluation of the susceptibility zonation, it must be considered that good validation does not necessarily correspond to good predictive power of the model. From a statistical point of view, the validation process is equivalent to the construction of two distinct models adopting two distinct landslide sets randomly extracted from the same population. So a high similarity between the two models merely reveals the stability, or non casuality, of the model itself, as the result does not change even if different landslide samples are adopted. As regards the predictive capacity of the model, a good validation simply means a good capacity to predict the observed landslides, i.e. the past ones. Instead, the reliability of the model in forecasting future landslides derives from the assumption that future landslides will occur at the same factor combinations and under the action of the same, in quality and quantity, triggering factors as in the past. The more recent the analyzed landslides are, the higher the probability is that they initiated in passive and active conditions analogous to those expected in the near future. For the shallow slides affecting the regolith that originate seasonally in substantial quantities following intense rainfall, the assumption holds. On the contrary, the deep-seated landslides that form more rarely and persist for a long time may be of an antique, often unknown age and so may have been produced in conditions that are substantially different from current ones. The introduction of these landslides into the analysis, as usually occurs owing to their importance in producing damage, reduces the predictive capacity of the model by an amount that is impossible to assess.

Good validation is a necessary but insufficient prerequisite for assessing the efficiency of a model. A good model should not only be reliably from a statistical point of view but should also be able to distinguish between significantly different landslide density conditions. So a good model should have a great spread or dispersion around the mean density value. Two very simple and intuitive statistical indices to quantify dispersion of data around the mean value exist: the mean deviation, i.e. the average absolute deviation from the mean, and the well known standard deviation. As the squaring in the standard deviation attaches great significance to the more extreme values, that often refer to the smaller and therefore less significant UCUS, the mean deviation seems more appropriate. In the shell script the mean deviation of the UCU density for each landslide type is computed. When more zonation models present acceptable and comparable validation values, the model with the highest mean deviation, and so with the greater differentiation capacity, should be preferred.

The shell script

The high number of GIS commands and the operational complexity has made an automation of the procedure through the creation of a shell (or program) script indispensable. In a previous work (Clerici et al. 2002), a relatively simple shell script was proposed for the construction of Landslide Susceptibility maps considering

the whole landslide surface, as proposed in the original formulation of the Conditional Analysis method. The subsequent adoption of the MSUE as the geomorphological feature representative of a landslide, made the procedure much more complex requiring a new specific shell script (Clerici 2002). In the current version other features have been added to the program, such as, for example, the possibility of performing susceptibility analysis separately for each landslide type and the model validation procedure.

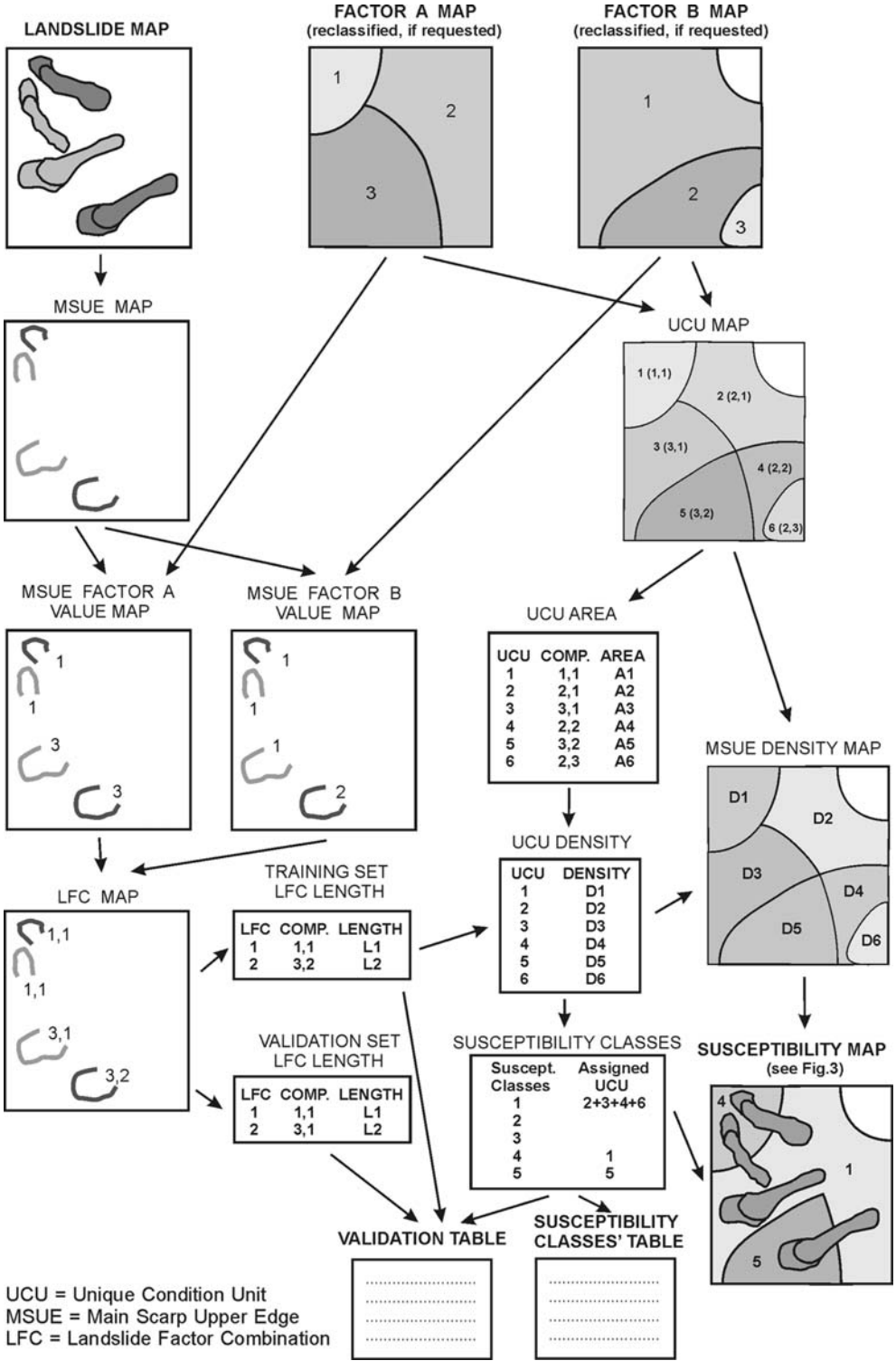

Fig. 3 Steps of the automated procedure for landslide susceptibility map construction. A simple case with only two factor maps and only four landslides, two for the training set (*dark gray*) and two for the validation set (*light gray*), is considered. The entire procedure is repeated for each landslide type

The script is mainly based on the GRASS GIS (Version 5.3) (GRASS Development Team 1999; Neteler and Mitasova 2004), a Free Software/Open Source system released under GNU General Public License and presently maintained by an international team with the official master site in Italy (http://www.grass.itc.it) and many mirrors all over the world.

In the script, commands of the Bash shell (Free Software Foundation 2002; Cooper 2005), of the text processing language 'gawk' (Free Software Foundation 2003) and of the non-interactive line editor 'sed' (Pizzini 1998) are also widely used. Considering that the script was implemented under Linux O.S., only free software has been used, making the procedure very inexpensive from an economical point of view.

The program requires as input a Landslide Inventory map containing all the landslides mapped in the study area and at least one, and up to a maximum of 10, factor maps. The output consists in a Job report containing two tables for each landslide type (see Table. 4, 5, 6, 7). The first table reports the characteristics of the five susceptibility classes, the second one the validation procedure results.

For each landslide type and/or for all the types as a whole, a map showing the five classes of landslide susceptibility and the current landslides can be displayed on the screen and/or output in Postscript format in any user selected scale (see Fig. 5 as an example). The map name, a legend, a graphic scale and a north arrow are also displayed. In the legend a sixth class is added if undefined areas are present.

Landslide susceptibility calculation

The steps of the entire procedure are schematically shown for a very simple theoretical case in Fig. 3. The first step is the reclassification (if requested) of the factor maps. The reclassified maps are then overlayed in order to obtain the UCU map, i.e. the map containing all the factor class combinations in the study area. Each combination is distinguished in the map by a different identification number, while the factor combination is stored as a category label (in brackets in the figure). If no value is defined in some portion of any factor map, as shown for the Factor B map in the figure, the corresponding area is excluded from the definition of the UCUs and therefore from the subsequent processing. From this map a file reporting the extension of each UCU in the investigated area is created (UCU area file).

Subsequently, the MSUEs are extracted from the main scarps in the Landslide Inventory map (MSUE map) (Fig. 1). The length (in meters) of each MSUE is then computed by summing the length of each cell. The total length of all MSUEs is then divided by the total area occupied by the UCUs to define the MSUE mean density, and by the MSUE number to define the MSUE mean length.

Afterwards, for each MSUE cell, the class value of each factor is defined by a paired analysis of the MSUE map and each single Factor map (Fig. 2). For each factor, a map is thus constructed in which the proper factor value is assigned to each MSUE cell. By overlaying these maps, the factor combination is defined for each MSUE cell and a landslide factor combination (LFC) map created.

Then, a file with the MSUE length (in meters) is created for each LFC of the training set and joined to the previously created file with UCU extensions; the resulting UCU Density file is used for the reclassification of the original UCU map leading to a new MSUE density map containing the MSUE density values expressed in m/km^2.

The Susceptibility Classes' file, obtained by assigning each UCU to the pertaining susceptibility class according to its MSUE density value, is then used to reclassify the MSUE density map, leading to the construction of the final landslide susceptibility map to which the 'undefined' areas (if any) and landslides are then superimposed. As already mentioned, the characteristics of this map are reported in a specific table in the job report.

For the validation procedure, a file with the MSUE length (in meters) is created for each LFC of the validation set (Validation Set LFC Length) and the length (in meters and in percent) of the validation set MSUEs falling in each previously defined susceptibility class, is computed. The absolute value of the difference with the percent of the MSUE length of the training set is reported in the validation table of the job report.

The Baganza basin susceptibility map construction

The described procedure has been applied to the mountainous and hilly part of the Baganza Torrent basin, in the Northern Italian Apennines, about 50 km south-west of Parma town (Fig. 4). The basin area is 167.386 km^2.

Geological framework

The Northern Apennine fold-and-thrust belt developed through the deformation of several sequences overthrusted during tectonic phases from Latest Cretaceous to Early Pleistocene. From Late Miocene, the Adria-verging Apennine belt was affected by extensional faulting, well developed in the Tuscan sector (Elter et al. 2003).

The Baganza valley (Fig. 4) cuts into the Po plain side of the Apennine chain in correspondence with a major transverse discontinuity affecting the belt. This tectonic discontinuity divides the Apennines into two segments characterized by a substantial difference in the tectonic uplift (Bernini et al. 1997). The NW portion of the belt is remarkably less uplifted compared with the SE portion; in fact, the Ligurian and Epi-Ligurian units overthrusting the Tuscan foredeep unit, outcrop extensively. On the contrary, in the south-eastern portion the Tuscan units form the Apennine backbone. This structural framework implies a regional NW dip of the bedding and is responsible for the pronounced asymmetry of the Baganza valley.

The uppermost part of the valley is located on the northern flank of an anticline affecting the Upper Oli-

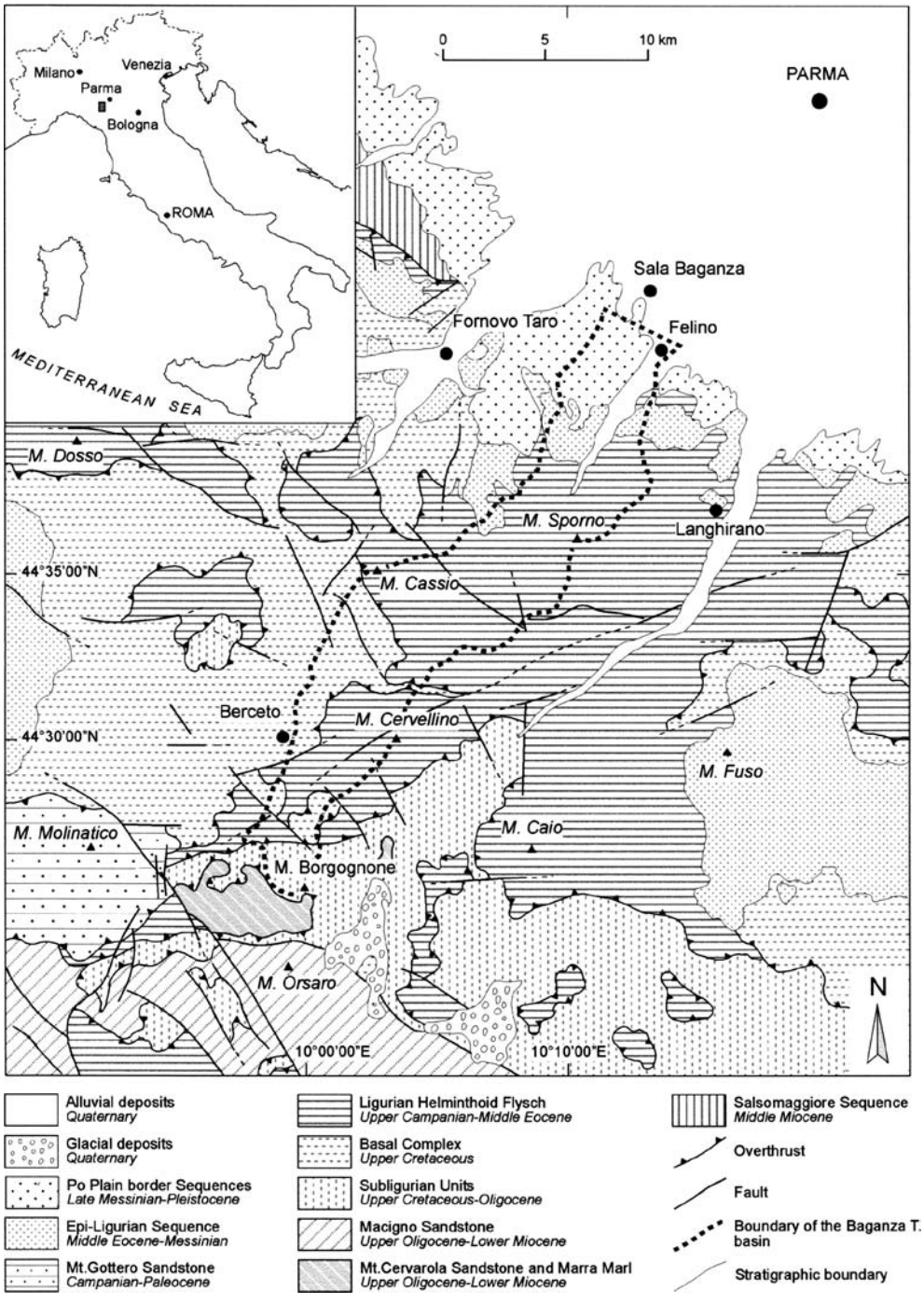

Fig. 4 Structural sketch of the sector of the Italian Northern Apennines including the Baganza basin

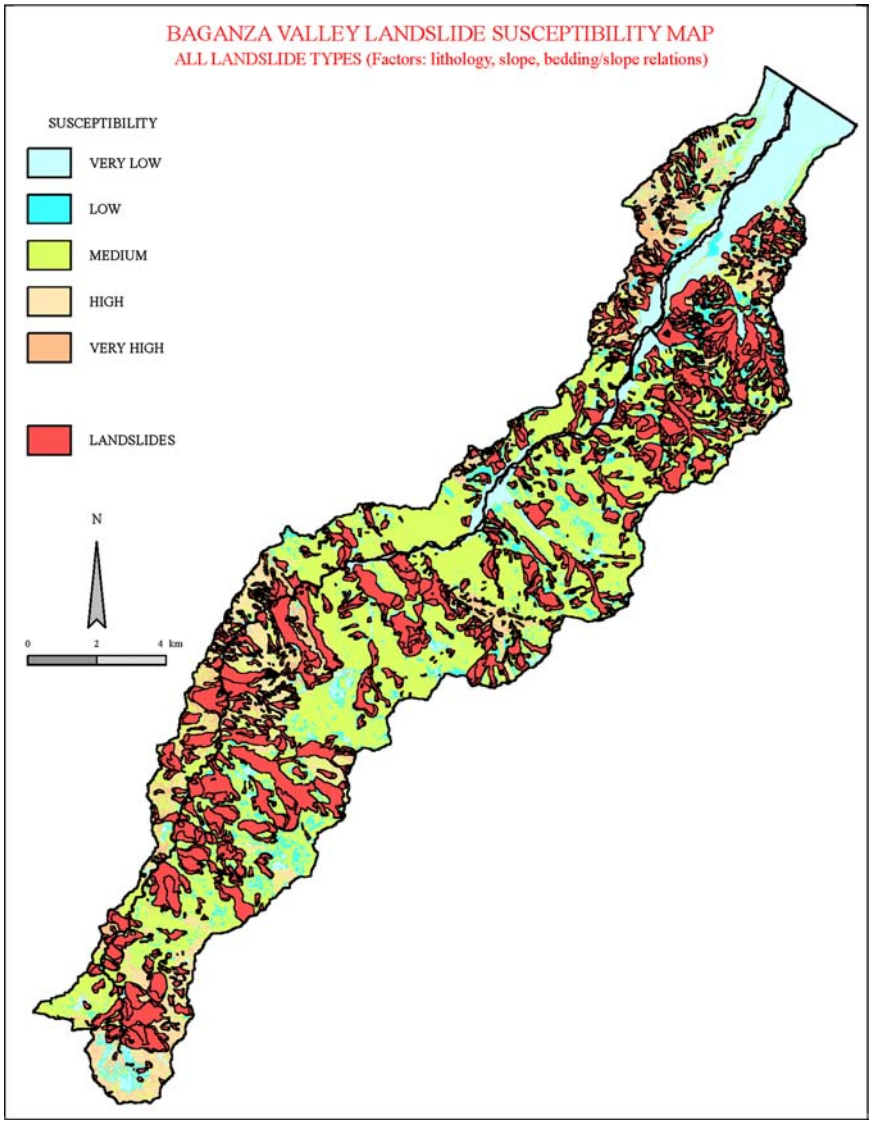

Fig. 5 Landslide susceptibility map of the Baganza basin obtained by the Conditional Analysis method applied to all landslide types with the factor combination 1-2-5 (lithology, slope angle, bedding/slope relations). The map was produced in Postscript format in A4 size

gocene-Lower Miocene foredeep turbidites overthrusted by the Subligurian Units, Upper Cretaceous-Oligocene in age (Vescovi 1998). The upper valley continues northward cutting the overthrusted Ligurian Units mainly consisting of the thick Helminthoid flysch sequences, made up of thick-bedded marly-limestone turbidites, Upper Campanian-Middle Eocene in age. Along the middle sector of the valley, the erosion has preserved extensive portions of the Basal Complex units consisting of Lower Cretaceous scaly clays with limestone, ophiolite bodies, Cenomanian-Santonian thin-bedded sandstone turbidites, and Campanian red shales (Vescovi et al. 1999). Along the lower sector of the Baganza valley the Early Cenozoic Flysch outcrops (Cerrina Feroni and Vescovi 2005); this unit shows a clay-rich upper portion, locally overlain by the Epi-Ligurian Sequence. In correspondence with the Apennine border, the Messinian continental conglomerates overlie the Early Cenozoic Flysch. The Messinian deposits are in turn overlain by the Plio-Quaternary marine sequence and by the Quaternary continental deposits (Di Dio et al. 1997).

Main geomorphological and climatic features

The Baganza valley develops in a SW–NE direction, from the Apennine reliefs of Mt Cervellino (1,492 m) and Mt Borgognone (1,400 m) to the hilly margin of the valley, near Felino village (Fig. 4). From here the Baganza torrent continues its course through the plain until it flows into the Parma river, in the town of Parma at an altitude of 58 m. The Baganza basin is particularly long and narrow with a length of about 34 km and a width

ranging from about 3 to 6 km. A relevant characteristic of the valley is the V-shaped cross profile, with a noticeable asymmetry: the eastern slope is much more extended than the left slope which is steeper with lower peaks. This asymmetry, uncommon in the Emilian Apennine basins, is conditioned by the structural setting, as specified in the previous section.

The landforms shaped by running waters and gravity prevail in the area. Locally, in the upper valley, Pleistocene glacial landforms are present; these relict landforms are, however, less evident in comparison with those in the adjacent valleys, as they developed in weak lithologies which were unsuitable to their preservation. Nevertheless, there is evidence of Pleistocene periglacial phenomena in block fields and cryogenic and nival hollows.

Impressive forms of differential erosion due to the presence of resistant rock units associated to weak rocks, are also frequent. The most striking example of is the NNW trending ''Salti del Diavolo'' conglomerate that outcrops across the middle valley with a thickness of about 15 m and a nearly vertical dip.

Nevertheless the clearly prevailing modeling is due to the landslides caused by the favorable lithological and structural characteristics of the bedrock. In the eastern side of the middle valley, wide landslides are present, some of which have been active for a long time. Many landslides are dormant and large in size; active landslides are lower in number and extension, yet they strongly influence the road conditions of the area. Among the recent reactivations, caused by a decade of intense autumnal precipitations (Bertolini and Pellegrini 2001), the most significant one is situated on the NW slope of Mt Cervellino where, on November 2000, a complex landslide was activated, with a length of 3.2 km, a width of 400 m and a presumed volume of about 40×10^6 m^3.

The Baganza valley is characterized by considerable climatic variation as regards both temperature and rainfall. Analysis of rainfall values registered in the stations of the valley and in adjacent areas makes it possible to define the yearly and monthly rainfall amount and the rainy days distribution. The yearly isohyets have values ranging from about 800 mm in the lower valley to 2,000–2,500 mm on the watershed (Bertolini and Pellegrini 2001). The monthly average rainfalls have a distribution with two maxima in late Autumn (usually November) and in Spring (March or April) and two minima in Winter (usually February) and in Summer (usually July). The distribution of the yearly rainy days shows a similar trend. The rainfall regime is therefore typical of the so-called ''sublitoraneo-appenninico'' climate affecting most of the Apennines in the Parma province (Pinna and Vittorini 1985). Orography plays an important role in the temperature distribution: the monthly temperatures indicates values of 13°C in the lower valley and 7–8°C on the main divide.

Input maps

The reliability of a susceptibility zonation is conditioned not only by the model adopted and the number and type of factors used in the analysis, but also by the quality of the collected data. The availability of detailed base maps and high-quality aerial-photographs, the systematic field check and the independent analysis of experienced investigators, can greatly reduce errors in data acquisition. However, irrespective of the experience and skill of operators a certain degree of uncertainty is always associated with the data (Carrara et al. 1995b). For example, in landslide mapping some boundaries can be difficult to identify due to erosional processes or human activity. In a geological map, the boundary between formations can be hidden by dense vegetation or detrital covers. Furthermore, maps constructed by numerical cartographic techniques, as for example Digital Elevation Models or slope maps, can be different if different algorithms or different grid resolutions are adopted. These unavoidable sources of uncertainty are incorporated in all the phases of the analysis and their influence on the final susceptibility zonation is difficult to quantify.

All the maps used in the analysis are in raster format. The large scale of the base maps, the quite limited extension of the study area and the reasonably short running time of the shell script allowed to adopt the pretty high resolution of 5 m. This cell side adequately describes also the smallest landslide of the area, whose MSUE length is about 35 m. The basin includes a total of 6,695,423 cells.

Landslide Inventory map

All the landslides were mapped at 1:10,000 scale by interpretation of aerial photographs of 1996 and 2001, at a scale of about 1:33,000 and 1:14,000, respectively, and by field verification. Six landslide types were distinguished according to the classification of Cruden and Varnes (1996): falls, translational slides, rotational slides, lateral spreads, flows and complex landslides.

The landslides are 1,147 and occupy an area of 56.5 km^2, representing the 33.8% of the whole basin. The different landslide types show very different frequencies. There is only one very small fall along the steep wall of an ophiolite body in the upper valley. Lateral spreads are only four, consisting of flysch blocks slightly shifted on the basal clayey complex. Five translational slides affect the flysch in those rare situations where strata are outward dipping with slope angle greater than dip angle. The rotational slides are 286 and affect many different rock formations, but especially the marly-limestone flysch and the thin-bedded sandstones and mudstones. They usually show a large detachment area and limited shifting of the depleted material. Earth

and mud flows are the most frequent landslide type totalling 443. They usually have small depletion areas with the channeled material converging on a common accumulation area. Complex landslides show the largest areal extent. Many of them are substantially rotational in the upper portion and evolve as flows in the toe, even if different landslide types are also present along the crown, especially falls and flows. When a single type of initial failure was clearly detectable, the landslide was assigned to the proper specific type; this is the case of many rotational/earth-flow complex landslides that were assigned to the rotational type. In the study area a total of 408 complex landslides was mapped.

With respect to the chronology of the landslides, on the basis of historical documentation (Boccia 1804; Almagià 1907; Dall'Olio 1975), local technical reports and newspaper chronicles, it was possible to date the movements of hundred of landslides in the Western Emilia Apennines. Furthermore, 71 ^{14}C age determinations referred to 36 landslides were carried out giving values ranging from 100 to 29,600 years B.P. Six of these radiometric dates regard the Mt Cervellino landslide, in the Baganza valley, and testify six movements in a time span from 1940 to 5730 years. B.P., i.e. from the Upper Atlantic to the Lower Subatlantic (Tellini and Chelli 2003). Obviously these dates generically refer to episodes of landslide activity and do not reveal the first movement age. Nevertheless they suggest that many landslides in the basin may be very old.

The maps were scannerized, imported into GRASS, rectified and georeferenced. The boundary of the main scarp and of the accumulation zone of each landslide were then digitized. In the editing phase, a specific numerical code was assigned to each different digitized feature: the first digit identifies the landslide element (main scarp or accumulation), the second the type of landslide and the remaining five digits are the progressive number of the element.

Only the landslide types with a significant presence, i.e. rotational slides, flows and complex landslides have been used for susceptibility analysis. For each of the three types, landslides have been randomly split into two groups, the training set, containing about the 75% of landslides and the validation set, with the remaining 25%.

Factor maps

Given that, as specified above, in the Baganza valley many landslides are probably very old, only time-invariant factors can be used. Among them, lithology and slope angle are globally acknowledged as the most important ones in affecting landsliding and are introduced in practically all works dealing with landslide susceptibility assessment since the work of Brabb et al. (1972). In the Baganza torrent area a detailed geological map at 1:10,000 scale, delivered also in digitized form by the Cartographic Office of the Regione Emilia Romagna and many recent geological maps (Cerrina Feroni et al. 1990; Andreozzi and Zanzucchi 1999; Vescovi 2002; Cerrina Feroni and Vescovi 2005) are available, making the construction of a lithological map a rather simple operation.

The same Cartographic Office also releases digitized contours lines with a contour interval of 5 m. Therefore a detailed digital elevation model (DEM), and subsequently a slope angle map, were easy to construct through the GRASS GIS commands. With the DEM it was immediately possible to construct two other morphometric characteristics which are often used in landslide susceptibility analysis: slope aspect, directly derived from the DEM, and elevation, represented by the DEM itself properly reclassified. These two layers, combined with the strata attitudes reported on the above mentioned geological maps, made possible the construction of a map portraying the bedding/slope relations. Therefore the following five factors were used in the analysis: lithology, slope angle, slope aspect, elevation and bedding/slope relations. In defining the LFCs a distance from the MSUEs of zero cells was adopted for lithology, whereas for the other four factors, calculated by a neighboring procedure, a distance of two cells was preferred.

Lithology

Geological maps in vector format of the area were joined, updated by the more recent geological surveys and transformed into raster format. In the area, there is an overall presence of 36 lithostratigraphic units and 15 drift cover types, for a total of 51 different units. In running the shell script, these were originally reduced to 15 lithological classes defined on the basis of the prevailing rock composition and the structural characteristics. As a bivariate analysis showed that three classes, namely gravel and sand deposits of the recent terraces, morainic and palustrine deposits, have no landslides, these were grouped in the same class in spite of their lithological and structural differences. So the final reclassed map was reduced to the following 13 categories: 1 = Surficial deposits; 2 = Talus deposits; 3 = Gravel and sand deposits of the recent terraces, morainic and palustrine deposits; 4 = Gravel and sand deposits of the old terraces; 5 = Clays with embedded limestone and serpentinite blocks; 6 = Marly-limestone flysch; 7 = Marly-clays; 8 = Thin-bedded sandstones and mudstones; 9 = Poorly cemented conglomerates; 10 = Scaly clays; 11 = Massive clays; 12 = Poorly cemented sandstones; 13 = Marls with discrete coherence.

The extension of the lithological classes and the MSUE lengths and densities for each landslide type are reported in Table 1. One evident characteristic is the presence of classes with extremely variable extension; class 6 (marly-limestone flysch) occupies over half of the area, whereas other lithologies show reduced extensions and therefore limited statistic significance, as for example class 12 with an area of only 0.66 km^2.

Considering the total of all the landslide types, a high density variability among the different lithologies is evident, with values ranging from nearly 0 in class 3 to over 2,000 m/km^2 in classes 7, 9 and 10. The high densities of classes 7 (2,568 m/km^2) and 10 (2,041 m/km^2) are justified by the presence of weak lithologies (clays and marls) affected by pervasive deformations that favor, in particular, the flow type. The latter presents the highest density values precisely in correspondence with the two classes 7 (987 m/km^2) and 10 (1,122 m/km^2). Complex landslides also show a high density (1,414 m/km^2) in correspondence with class 7, but a maximum (1,921 m/km^2) in the poorly cemented conglomerates of class 9. The rotational landslides, on the other hand, present high values in the thin-bedded turbidites of class 8 (455 m/km^2) and in the talus deposits of class 2 (500 m/km^2). The paltry densities of classes 3 and 4 are obviously justified by the flat morphology of the terraces and not by the lithological characteristics.

Table 1 Area and main scarp upper edge (MSUE) length (in m) and density (in m/km^2) for each landslide type in the classes of the 5 factors used in the analysis

F	C	Area		Rotational		Flow		Complex		All types	
		km^2	(%)	Length	Density	Length	Density	Length	Density	Length	Density
1	1	7.5	4.5	918	122	1,526	203	1,942	258	4,386	584
	2	1.0	0.6	514	500	552	537	677	659	1,743	1,697
	3	6.1	3.6	6	1	13	2	0	0	19	3
	4	7.8	4.7	702	90	168	22	0	0	870	112
	5	15.1	9.0	5,127	339	9,696	641	10,531	696	25,354	1,515
	6	96.7	57.8	28,154	291	22,772	235	66,138	684	117,064	1,210
	7	3.9	2.3	648	166	3,862	987	5,529	1,414	10,039	2,568
	8	14.9	8.9	6,775	455	6,309	424	1,1787	792	2,4871	1,671
	9	1.5	0.9	437	294	212	143	2,853	1,921	3,502	2,358
	10	4.2	2.5	676	159	4,754	1,122	3,218	760	8,648	2,041
	11	6.3	3.7	1,012	162	2,400	384	6,122	979	9,543	1,525
	12	0.7	0.4	275	418	418	635	0	0	693	1,053
	13	1.7	1.0	337	203	599	361	154	93	1,090	658
2	1	22.1	13.2	1,242	56	1,695	77	5,224	237	8,161	370
	2	29.7	17.7	4,521	152	8,409	283	16,119	543	29,049	979
	3	35.3	21.1	7,997	226	15,508	439	25,463	721	48,968	1,386
	4	27.8	16.6	8,177	294	11,357	409	22,479	809	42,013	1,512
	5	17.9	10.7	7,414	413	6,338	353	14,869	829	28,621	1,595
	6	14.3	8.6	6,678	466	4,746	331	1,0445	728	21,869	1,525
	7	9.1	5.4	4,292	474	2,594	286	6,442	711	13,328	1,470
	8	11.2	6.7	5,259	470	2,632	235	7,910	707	15,801	1,411
3	1	27.6	16.5	6,540	237	7,226	262	19,234	697	33,000	1,196
	2	26.3	15.7	8,075	307	7,860	298	17,032	647	32,967	1,252
	3	15.7	9.4	6,560	419	5,187	331	8,504	543	20,242	1,293
	4	14.1	8.4	5,881	418	6,028	428	8,529	606	20,439	1,453
	5	9.7	5.8	2,004	207	4,186	432	6,043	624	12,227	1,263
	6	19.4	11.6	4,182	215	6,572	338	1,1843	610	22,572	1,162
	7	22.5	13.4	4,597	204	7,133	317	15,022	668	26,742	1,189
	8	32.0	19.1	7,706	241	9,088	284	22,556	704	39,350	1,229
4	1	35.1	21.0	3,501	100	9,620	274	18,744	533	31,865	907
	2	27.6	16.5	6,589	239	11,786	428	21,787	791	40,162	1,457
	3	35.8	21.4	10,361	289	12,722	355	19,457	543	42,540	1,188
	4	32.2	19.2	12,624	393	12,959	403	24,918	775	50,501	1,571
	5	24.2	14.5	8,552	353	4,349	179	14,867	613	27,768	1,146
	6	12.5	7.5	3,954	317	1,845	148	9,178	735	14,977	1,199
5	1	62.8	37.5	18,692	297	17,420	277	46,888	746	83,000	1,321
	2	43.0	25.7	12,604	293	11,200	261	27,457	639	51,261	1,193
	3	10.0	6.0	5,047	505	1,836	184	7,802	781	14,685	1,470
	4	51.6	30.8	9,236	179	22,824	443	26,804	520	58,864	1,142

F Factor (*1* Lithology, *2* Slope angle, *3* Aspect, *4* Elevation, *5* Bedding/slope relations), *C* Classes

In spite of the above mentioned limits of the bivariate analysis, these simple observations confirm that lithology exerts a substantial control on the landslide density and type.

Slope angle

The original slope values, ranging from 0° to 77.3°, were reclassified with the shell script in the following eight categories with an interval of 5°: 1 = 0–5°; 2 = 6–10°; 3 = 11–15°; 4 = 16–20°; 5 = 21–25°; 6 = 26–30°; 7 = 31–35°; 8 = >35°.

The extension of the classes and the MSUE lengths and densities for each landslide type are reported in Table 1. The adopted class interval brought a good subdivision of the study area as the minimum class extension is big enough, 5.42%, to allow a statistical analysis. Analyzing the density values for all landslide types, the central classes 4, 5, 6, with a slope angle ranging from 16 to 30° present the highest density values. Yet, except for the two lower classes (from 0 to 10°), the differences are not particularly significant. The situation is different for the different landslide types. In fact the rotational slides show a constant density increment along with the increase in steepness, reaching the maximum in classes 6, 7 and 8, whereas the complex landslides show their highest density in classes 4 and 5; finally, the flows have their maximum in classes 3 and 4. It is therefore evident that flows generate in correspondence with low slope angle values, while rotational slides require higher values. Complex landslides are generated in intermediate steepness conditions. As it was already observed for lithology, this factor also reveals a strict relationship with landslide density and type.

Slope aspect

If the significance of the previous factors meet with current research results, the meaning of slope aspect in explaining instability is still debated as different conclusions are drawn by different authors in different areas and with different techniques. It is generally accepted that slope orientation affects the exposure to sunlight and to winds, affecting indirectly other factors that contribute to landslides, such as precipitation, soil moisture, vegetation cover and soil thickness. Most authors agree in considering that at middle and high latitudes the N and NW-facing slopes (or S-facing in the southern hemisphere) are the most favorable to landsliding due to their shadier and colder conditions that favor the accumulation of snow, a higher moisture content for a longer time and a greater physical weathering (Carrara et al. 1991; Lineback Gritzner et al. 2001; Fernandes et al. 2004; Lan et al. 2004; Lee et al. 2004; Tangestani 2004; Moreiras 2005). It is worth noting that in other studies drier slopes result more favorable to landsliding (Dai and Lee 2002; Perotto-Baldiviezo et al. 2004; Shresta et al. 2004). For other authors the high landslide density on specific slope orientation is connected to local conditions as for example the prevailing direction of winds and storms, the rock structure and fault orientation, or even the coastal erosion (Larsen and Torres-Sánchez 1998; Jakob 2000; Lin and Tung 2003; Fernandes et al. 2004; Ayalew and Yamagishi 2005). Finally, others authors, in different areas, did not notice significant relationships between landslides and aspect (Çevik and Topal 2003; Ohlmacher and Davis 2003; Ayalew and Yamagishi 2004), while Atkinson and Massari (1998) found aspect significant for larger and older dormant landslides, but not for active ones and for Luzi and Pergalani (1999) aspect shows an influence on rotational slides, but not on flows and translational slides.

In the study area, slope aspect has been divided in 9 classes. Classes from 1 to 8 represent the eight angular sectors 45° wide, whose bisectors correspond to the main and the secondary cardinal directions; the last class contains the horizontal cells. The class intervals (values in degrees, clockwise from north) are the following: 1 = 337.6-22.5 (N); 2 = 22.6–67.5 (NE); 3 = 67.6–112.5 (E); 4 = 112.6–157.5 (SE); 5 = 157.6–202.5 (S); 6 = 202.6–247.5 (SW); 7 = 247.6–292.5 (W); 8 = 292.6–337.5 (NW); 9 = horizontal.

This factor poses a special problem as the last class, whose extension is only 0.1 km^2 corresponding to the 0.06% of the area, does not really contain an aspect value, but groups together all the cells whose orientation cannot be determined. For this reason it was excluded from the analysis during the reclassification phase. The extension of the classes and the MSUE lengths and densities are reported in Table 1.

If we consider all landslides, the class densities do not show a significant variability, as values range from 1,162 to 1,453. Some small differences can be noted for rotational slides showing higher values in classes 3 and 4 (E and SE) and for flows with prevailing densities in classes 4 and 5 (SE and S). So this factor, if taken alone, does not seem to have good explanatory power of landslide distribution.

Elevation

In general slope failures are considered more frequent at higher altitudes because of the increase in rainfall and snowfall and the strength of freeze-thaw cycles. This relationship is confirmed in some studies (Lin and Tung 2003; Menéndez Duarte and Marqínez 2002), whereas in many other cases, usually due to the interference of other factors such as lithology, different relationships are found; for example in Dai and Lee (2002), Zhou

et al. (2002), Çevik and Topal (2003), Ayalew et al. (2004), Lan et al. (2004), landslides are mostly distributed in areas belonging to lower and/or middle elevation classes. In other studies elevation is shown to have little impact on the occurrence of landslides (Guzzetti et al. 1999; Lineback Gritzner et al. 2001; Ayalew and Yamagishi 2005).

The elevations in the basin, ranging from a minimum of 169 m to a maximum of 1,492 m., were reclassified adopting a class interval of 200 m in the following 6 classes: 1 = 169–400; 2 = 401–600; 3 = 601–800; 4 = 801–1,000; 5 = 1,001–1,200; 6 = 1,201–1,492. The results of the bivariate analysis are reported in Table 1. Density distribution does not present a significant trend to indicate a strict relationship between elevation and landslide density. In fact the highest values are found in classes 2 and 4 while the low values of class 1 are strongly influenced by the presence of ample and stable terraced surfaces in the terminal part of the basin. It is evident therefore that the different densities are attributable to other conditions only partly connected to elevation, confirming that this factor has a poor direct relationship with landsliding, at least in the investigated area.

Bedding/slope relations

The structural setting is usually considered as affecting the slope stability, with a different degree of landsliding strictly connected to the geometric relationship between bedding attitude and slope (Cruden and Hu 1996). However this factor is rarely introduced into the analysis (Atkinson and Massari 1998; Guzzetti et al. 1999; Donati and Turrini 2002; D'Amato Avanzi et al. 2004; Ercanoglu and Gokceoglu 2004; Ayalew and Yamagishi 2005) probably due to the difficulty in the acquisition of large sets of reliable attitude data to adequately represent the structural setting and to the lack of a satisfactory procedure for the transformation of point data to a continuous surface. The results of statistical analysis are not univocal. For example Carrara et al. (1991) found that beds dipping toward the free face facilitate mass-movement and D'Amato Avanzi et al. (2004) discovered that downslope class shows the highest landslide presence, but in the area investigated by Atkinson and Massari (1998) landsliding is unrelated to the strata/slope relation and for Donati and Turrini (2002) layers dipping opposite to the slope have a greater incidence on landsliding than dip-with-slope layers.

Some years ago a GIS based procedure was implemented in order to define different situations by combining the bedding attitude (dip angle and direction) with slope geometry (slope angle and aspect) (Clerici et al. 1993). Examples of the use of the procedure can be found in Clerici et al. (2002), Donati and Turrini (2002) and Bednárik et al. (2005). The resulting 13 different bedding-slope situations are reported in Table 2.

The procedure was applied by using 1,225 attitude data reported for the study area in the already mentioned detailed geological maps at 1:10,000 scale. By a reclassification operation, classes 1 and 2 (horizontal and vertical strata) that occupy only 0.21 and 0.33%, were incorporated into class 3 (inward dipping strata), of which they represent the two opposing extremes, to form a single class (new class 1). Class 4, that occupies about a quarter of the entire area, was reclassified as new class 2 (cataclinal under-dip). A third new class includes all classes from 5 to 13 (cataclinal over-dip) that occupy overall only the 5.97% of the whole area. Finally, all lithologies without stratification, with an undefined stratification, or which are strongly deformed, were put into the new class 4. In summary, the resulting four reclassified classes are: 1 = horizontal, vertical and inward dipping strata; 2 = outward dipping strata with slope angle less than dip angle; 3 = outward dipping strata with slope angle greater than dip angle; 4 = non-bedded or strongly deformed formations.

In Table 1 the extension of the four classes and their MSUE lengths and densities are listed. Considering all landslides types (last column) there are no substantial differences in the density values, ranging from 1,142 to 1,470 m/km^2. Much more meaningful are the results for each single landslide type. In fact, the rotational slides have a predominant density (505 m/km^2) in class 3, according to the common opinion of a greater instability of slopes with outward dipping strata and slope angle greater than dip angle. Flows indeed show a predominant density (443 m/km^2) in class 4 containing formations with no stratification, that are mainly the clayey, or at least the clayey predominant, units. Complex landslides are less differentiated even if higher densities are

Table 2 Classes of bedding/slope relations

Class	α(°)	β(°)	γ(°)	Bedding/slope relations
1	0–5	Any	Any	Horizontal strata
2	85–90	Any	Any	Vertical strata
3	5–85	>90	Any	Anaclinal (inward dipping)
4	5–85	<90	<0	Cataclinal under-dip (outward dipping with slope angle less than dip angle)
5	5–30	0–10	>0	Cataclinal over-dip (outward dipping with slope angle greater than dip angle)
6	5–30	10–60	>0	
7	5–30	60–90	>0	
8	30–60	0–10	>0	
9	30–60	10–60	>0	
10	30–60	60–90	>0	
11	60–85	0–10	>0	
12	60–85	10–60	>0	
13	60–85	60–90	>0	

The 13 classes are defined by different combinations of α, the slope angle, β, the difference between slope direction and strata direction, and γ, the difference between slope angle and dip angle. The terms anaclinal and cataclinal (over-dip and under-dip) are taken from Ayalew and Yamagishi (2005)

Table 3 Results of the procedure application to the 31 factor combinations

FC	TNU	ANU		R	F	C	A
1	13	13	VE	15.9	7.8	13.2	7.7
			MD	126	266	434	275
2	8	8	VE	3.5	7.2	2.4	3.8
			MD	137	81	135	118
3	8	8	VE	45.0	7.6	0.0	5.3
			MD	75	47	42	55
4	6	6	VE	25.6	17.5	0.6	11.4
			MD	75	98	102	92
5	4	4	VE	7.0	2.0	3.5	3.8
			MD	93	76	92	87
1-2	104	104	VE	11.0	6.1	10.1	8.8
			MD	275	341	506	374
1-3	104	104	VE	39.8	7.9	11.0	12.2
			MD	230	364	493	362
1-4	78	56	VE	22.6	13.8	17.2	14.5
			MD	216	433	656	435
1-5	52	28	VE	8.3	4.6	12.3	6.6
			MD	264	430	704	466
2-3	64	64	VE	27.4	7.7	7.1	5.9
			MD	158	100	182	147
2-4	48	48	VE	26.8	7.2	5.0	10.7
			MD	119	148	158	142
2-5	32	31	VE	7.5	9.4	5.0	4.2
			MD	137	157	156	150
3-4	48	48	VE	60.7	9.7	1.7	10.3
			MD	142	133	144	140
3-5	32	32	VE	31.6	10.3	10.1	6.3
			MD	124	105	149	126
4-5	24	24	VE	18.2	17.0	7.8	12.6
			MD	120	189	162	157
1-2-3	832	830	VE	37.5	12.4	15.0	17.2
			MD	409	465	711	528
1-2-4	624	437	VE	39.6	12.0	18.7	17.8
			MD	361	496	979	612
1-2-5	416	210	VE	17.9	5.8	11.6	9.3
			MD	432	554	988	658
1-3-4	624	443	VE	56.2	20.3	25.5	25.0
			MD	305	568	1,032	635
1-3-5	416	222	VE	33.4	10.0	17.1	14.6
			MD	573	975	1,372	973
1-4-5	312	113	VE	29.7	14.5	21.0	20.7
			MD	497	1,769	3,590	1,952
2-3-4	384	384	VE	48.1	7.7	10.4	12.1
			MD	290	405	550	415
2-3-5	256	248	VE	26.7	8.9	8.75	9.3
			MD	387	330	291	336
2-4-5	192	185	VE	26.4	19.2	12.5	15.7
			MD	254	293	279	275
3-4-5	192	192	VE	60.9	21.6	20.9	28.5
			MD	219	280	325	275
1-2-3-4	4992	3335	VE	66.1	37.5	35.5	40.6
			MD	695	676	1,341	904
1-2-3-5	3328	1612	VE	40.0	21.4	17.7	23.9
			MD	778	722	1,829	1,110
1-2-4-5	2496	807	VE	41.1	21.4	26.1	25.9
			MD	570	1,026	4,446	2,014
1-3-4-5	2496	824	VE	69.2	33.4	38.3	39.4
			MD	553	1,080	2,338	1,324
2-3-4-5	1536	1464	VE	66.8	46.4	44.7	47.4
			MD	384	393	579	452
1-2-3-4-5	19968	5567	VE	87.4	56.2	55.8	60.4
			MD	683	646	1,866	1,065

FC Factor combination (*1* Lithology, *2* Slope angle, *3* Aspect, *4* Elevation, *5* Bedding/slope relations), *TNU* Teorethical number of UCUs, *ANU* Actual number of UCUs, *R* Rotational slides, *F* Flows, *C* Complex landslides, *A* All types, *VE* Validation error, *MD* Mean deviation

reported in the landslide prone class 3 and in the theoretically more stable inward dipping strata of class 1.

Procedure application and analysis of the results

The procedure was applied considering each of the five single factors and all the possible 2-3-4-5-factor combinations, leading to the construction of 31 different models of susceptibility zonation. The results are summarized in Table 3 where, for each factor combination, the theoretical number of UCUs (number of all the possible factor class combinations) and the actual number of UCUs (number of combinations actually present in the area) are reported. For each landslide type and for the total of all landslides, the validation error (VE) and the mean deviation (MD) of the UCUs density values, are also listed.

If all landslide types are considered indistinctly, an analysis of the table reveals that, in general, the goodness of validation decreases with the increase of the number of factors introduced into the analysis. In fact, whilst the models with a single factor have a VE varying from a minimum of 3.8 to a maximum of 11.4, the combinations with four factors have values ranging from 23.9 to 47.4, with a maximum value of 60.4, for the combination of all five factors. This result is predictable considering that most of the factors are strictly related to each other, providing redundant information, as is highlighted by the reduction of the number of UCUs present in comparison with potential UCUs. Thus the introduction of a large number of factors does not significantly increase the amount of information fed into the model, but rather increases the number of small UCUs, which are not very meaningful from a statistical point of view. This confirms what was shown by Carrara and others (1995a, b) and Guzzetti et al. (1999), for whom an intrinsic limitation of any multivariate analysis is that as the number of variables increases the reliability of the model decreases to some extent.

Table 4 Job report for the factor combination 1-2-5 (lithology, slope angle, bedding/slope relations) applied to all landslides

Class	Class intervals and extension				Validation table				
	Class interval		Extension		Train. set		Valid. set		
	(m/km^2)	(N/km^2)	(km^2)	(%)	MSUE (m)	Length (%)	MSUE (m)	Length (%)	Diff. (%)
1 Very low	0–496	0.0–1.9	16.81	10.0	3,134	1.53	2,364	2.96	1.43
2 Low	497–993	1.9–3.9	11.54	6.9	23,201	11.30	9,676	12.11	0.81
3 Medium	994–1489	3.9–5.8	62.49	37.3	88,725	43.23	36,439	45.62	2.39
4 High	1,490–1,986	5.8–7.8	11.84	7.1	42,379	20.65	15,254	19.10	1.55
5 Very high	> 1,986	> 7.8	8.18	4.9	47,819	23.30	16,145	20.21	3.08
Landslides			56.53	33.8					
		Total	167.39	100.0	205,258	100.00	79,881	100.00	9.27

Also, the dispersal of the density values, expressed quantitatively by the MD, increases with the number of included factors. This characteristic is also obvious since it is connected to the increase of the UCU number. The low MD values relative to the single factor analysis, testify a scarce differentiation capacity. These models produce landslide density values that differ little from the average density and therefore lead to the absence in the examined area of the extreme density classes. This is particularly evident in the case of factor 5 (bedding/slope relations) as the number of UCU, corresponding to the number of factor classes (4), produce only four densities, less than the number of susceptibility classes (5). Also in the case of factor 1 (lithology), that shows the highest number of classes (13) and the higher MD (275), the very low and very high densities are scarcely represented.

It is evident that a good compromise between a good validation and a high differentiation can be found in the 2 and 3-factor combination models. This is confirmed by the fact that all the 2-factor models show very good validations, with VE from 4.2 in the combination 2-5, to 14.5 in the combination 1-4, and an MD from 126 to 466. In the 3-factor models the VE is generally higher, and the MD much larger ranging from 275 to 1,952. However, two combinations, namely the 1-2-5 and 2-3-5, present a very low VE, 9.3, which is comparable to the VE of the 2-factor models, and the first of them a noticeably higher MD value, 658. So the 1-2-5 combination (lithology, slope angle, bedding/slope relations) appears as the best compromise between a good validation level and a good dispersion of the density values and the more suitable for the landslide susceptibility zonation. The relevant report is represented in Table 4 and the Landslide Susceptibility map in Fig. 5.

As regards the single landslide types, the models for rotational landslides show bad validation values not only in the 4 and 5-factor combinations, but also in the 3-factor combinations, with a minimum value of 17.9 (1-2-5). The best results are in the 2-factor combinations, with a minimum value of 7.5 in the 2-5 combination and a slightly higher value of 8.3 in the 1-5 combination. Considering the higher MD (264 against 137), the latter model should be used for landslide susceptibility zonation relative to rotational landslides only (Table 5).

Flows show the lowest VE values, with the best results in the 2 and 3-factor combinations. The lowest value of 4.6, with a MD of 430, is in the combination 1-5, but the combination 1-2-5 also gives a very low value of 5.8 with a remarkably higher MD of 554. So this last model seems more suitable for a susceptibility zonation of flow typology (Table 6).

As regards the complex landslides, many 2-factor models show very good validations, as the combinations 2-3, 2-4, 2-5, 3-4, with a VE respectively of 7.1, 5.0, 5.0, 1.7, but low MD values ranging from 144 to 182. On the contrary the 3-factor combination 1-2-5, in spite of a

Table 5 Job report for the factor combination 1-5 (lithology, bedding/slope relations) applied to rotational slides

Class	Class intervals and extension				Validation table				
	Class interval		Extension		Train. set		Valid. set		
	(m/km^2)	(N/km^2)	(km^2)	(%)	MSUE (m)	Length (%)	MSUE (m)	Length (%)	Diff. (%)
1 Very low	0–108	0.0–0.5	14.60	8.7	717	1.58	111	0.82	0.76
2 Low	109–217	0.5–1.0	12.71	7.6	3,352	7.37	1,225	9.00	1.63
3 Medium	218–326	1.0–1.5	66.09	39.5	28,525	62.71	8,723	64.04	1.33
4 High	327–435	1.5–2.1	4.93	3.0	3,261	7.17	498	3.66	3.51
5 Very high	> 435	> 2.1	12.53	7.5	9,633	21.18	3,025	22.21	1.04
Landslides			56.53	33.8					
		Total	167.39	100.0	45,580	100.00	13,620	100.00	8.27

Table 6 Job report for the factor combination 1-2-5 (lithology, slope angle, bedding/slope relations) applied to flows

Class	Class intervals and extension				Validation table				
	Class interval		Extension		Train. set		Valid. set		
	(m/km^2)	(N/km^2)	(km^2)	(%)	MSUE (m)	Length (%)	MSUE (m)	Length (%)	Diff. (%)
1 Very low	0–127	0.0–0.7	19.18	11.5	812	1.56	683	2.96	1.40
2 Low	128–254	0.7–1.5	41.89	25.0	13,465	25.79	5,945	25.71	0.08
3 Medium	255–381	1.5–2.2	30.17	18.0	13,780	26.39	5,630	24.35	2.05
4 High	382–509	2.2–2.9	4.10	2.5	2,997	5.74	1,645	7.12	1.38
5 Very high	> 509	> 2.9	15.52	9.3	21,156	40.52	9,167	39.64	0.88
Landslides			56.53	33.8					
		Total	167.39	100.0	52,210	100.00	23,125	100.00	5.79

higher, but in any case low, VE of 11.6 has a much more better MD of 988. For this reason the 1-2-5 model, whose characteristics are reported in Table 7, seems to be more suitable for the susceptibility zonation of complex landslides.

In summary, the 1-2-5 factor combination is the best model for susceptibility zonation for all the landslides considered together and for flows and complex landslides. The combination 1-5 appears to be the best for rotational landslides. As regards the contribution of each single factor, it is interesting to note that in the best 2 and 3-factor models, factor 5, (slope/bedding relations), is always present (combinations 1-5, 2-5, 3-5, 1-2-5, 2-3-5). Factor 2 (slope angle) shows to be relevant in many models, especially if combined with factor 5 (2-5, 1-2-5, 2-3-5). Factor 3 (aspect) appears in three combinations (3-5, 2-3, 2-3-5) and factor 1 (lithology) is present in the best 1-2-5 and 1-5 models, but it gives unsatisfactory contributions in all the other combinations. The less significant factor is factor 4 (elevation): whether considered alone or combined with other factors, it always presents a bad validation level.

An idea of the effects of changing or adding a factor in a model can be had by comparing the resulting susceptibility maps. For example, the comparison between the two best 3-factor combinations, namely 1-2-5 and 2-3-5, offers the opportunity to evaluate the difference between two maps obtained by changing a single factor, namely factor 1 with factor 3, while the comparison between the 1-5 model, the best among the 2-factor combinations, and the 1-2-5 model, makes it possible to evaluate the effects of introducing one more factor, namely factor 2. In order to assess the differences, the landslide susceptibility maps were subtracted from each other obtaining a difference equal to 0 where the class values coincide in both the maps, a value of 1 for one class difference, and so on to a maximum value of 4, where the class value is 1 in a map and 5 in the other one. In Table 8 the areas of the resulting difference classes are reported. In the first comparison, about the 49% of the area has the same class values in both maps, while the difference of one class affects about the 43% of the area. A difference greater than 2 has an area of only the 1.4%. In the second comparison, the class 0 has an area of about 74% and the class 1 of about 23%, while the higher classes 2, 3 and 4 together are slightly greater than 3%. As expected, the three maps do not exhibit drastic differences mainly as a consequence of the strict relationship among the factors involved.

Regarding the running time, the complete analysis consisting in the construction of the susceptibility map for each of the three landslide types and for all the types considered together, required a minimum of about four hours for the models with only one factor, and a maxi-

Table 7 Job report for the factor combination 1-2-5 (lithology, slope angle, bedding/slope relations) applied to Complex landslides

Class	Class intervals and extension				Validation table				
	Class interval		Extension		Train. set		Valid. set		
	(m/km^2)	(N/km^2)	(km^2)	(%)	MSUE (m)	Length (%)	MSUE (m)	Length (%)	Diff. (%)
1 Very low	0–260	0.0–0.7	19.61	11.7	1,602	1.48	844	1.95	0.46
2 Low	261–520	0.7–1.4	3.86	2.3	2,646	2.45	1,471	3.40	0.94
3 Medium	521–781	1.4–2.1	62.30	37.2	65,932	61.09	28,324	65.33	4.25
4 High	782–1,041	2.2–2.8	17.69	10.6	21,976	20.36	7,893	18.21	2.15
5 Very high	> 1,041	> 2.8	7.40	4.4	15,774	14.62	4,691	10.82	3.79
Landslides			56.53	33.8					
		Total	167.39	100.0	108,950	100.00	43,353	100.00	11.60

Table 8 Differences between susceptibility maps 1-2-5 and 2-3-5 and between 1-5 and 1-2-5

	Class difference									
	0		1		2		3		4	
	km^2	%	km^2	%	km^2	%	km^2	%	km^2	%
125–235	54.43	49.10	47.58	42.92	7.31	6.59	1.40	1.27	0.14	0.13
15–125	82.43	74.35	24.97	22.53	1.80	1.62	1.59	1.44	0.68	0.06

mum of six hours for the 5-factor model, with a Pentium III 1,000 MHz with a RAM of 256 MB.

Conclusions

The main advantage of the Conditional Analysis method applied to the Unique Condition Units is its conceptual simplicity. The implementation of an automated procedure through a shell script makes the method fast and free of operational errors, making it possible to construct landslide susceptibility maps for wide areas quickly and with high resolutions, adopting different factor combinations and analyzing separately the different landslide types, as performed for the Baganza basin. Furthermore, the adoption of the open source GRASS GIS and other free software makes the procedure inexpensive.

The validation procedure furnishes a valuable method to assess the statistical reliability of landslide susceptibility zonation and the mean deviation a practical index to evaluate the UCUs' capacity to differentiate the landslide density values. The application of the procedure to the Baganza basin, has confirmed the importance of lithology and slope angle in explaining landslide occurrence, especially if associated with slope/bedding relation factor, even though it can not be excluded that the introduction of other factors could give similar or even better results.

For a correct evaluation of the results it must be considered that the reliability of the final map in predicting future failures depends strictly on two basic assumptions:

1. the cells at, or close to, the main scarp upper edge of a landslide are effective in representing the situation before the failure occurrence;
2. failures in the future will take place under the same conditions, defined by conditioning and triggering factors, which led to past instability, and consequently the predictive capacity relies on the age of landslides used for the model construction. If a chronological distinction of the landslides is not possible and very old landslides are also introduced into the analysis, as it was the case of the present work, only time invariant factors should be used, and the probability of a difference between past and future conditions increases, reducing the predictive power of the model by an indefinable amount.

Acknowledgements In this paper, A. Clerici was responsible for the procedure for landslide susceptibility zonation, S. Perego for geomorphological and climatic characteristics, C. Tellini for the landslide survey and mapping, P. Vescovi for the geological and lithological aspects. This study was supported partly by funds of the Parma University research project FIL 2004 "Evoluzione geomorfologica tardo-quaternaria: casi di studio nelle Alpi Marittime e nell'Appennino settentrionale" (Coordinator S. Perego), and partly by the COFIN 2002, National Research Program: "Evoluzione geomorfologia dei versanti e cambiamenti climatici: analisi di fenomeni franosi e ricostruzioni paleoclimatiche" (National coordinator M. Soldati); Local Research Program: "Cambiamenti climatici tardo-quaternari e instabilità dei versanti nell'Appennino settentrionale" (Local coordinator C. Tellini). Thanks to M. Gallarotti and A. Ruffini for help in data acquisition and editing, D. Peis for his kind assistance in solving computer problems, E. Masini for drawing some of the figures and P. Sears for valuable aid in translation. We are grateful to M. Soldati for detailed and helpful comments and suggestions.

References

Aleotti P, Chowdhury R (1999) Landslide hazard assessment: summary review and new perspectives. Bull Eng Geol Env 58:21–44

Almagià R (1907) Studi geografici sulle frane in Italia. Mem Soc Geogr It 13:1–342

Andreozzi M, Zanzucchi G (1999) Carta Geologica della Val Baganza. Scala 1: 50.000. STEP, Parma

Atkinson PM, Massari R (1998) Generalised linear modelling of susceptibility to landsliding in the central Apennines, Italy. Comput Geosci 24:373–385

Ayalew L, Yamagishi H (2004) Slope failure in the Blue Nile basin, as seen from landscape evolution perspective. Geomorphology 57:95–116

Ayalew L, Yamagishi H (2005) The application of GIS-based logistic regression for landslide susceptibility mapping in the Kakuda-Yahiko Mountains, Central Japan. Geomorphology 65:15–31

Ayalew L, Yamagishi H, Ugawa N (2004) Landslide susceptibility mapping using GIS-based weighted linear combination, the case in Tsugawa area of Agano River, Niigata Prefecture, Japan. Landslides 1:73–81

Bednárik M, Clerici A, Tellini C, Vescovi P (2005) Using GIS GRASS in evaluation of Landslide Susceptibility in Termina valley in the Northern Apennines (Italy). In: Proceedings of the 15th conference engineering geology, Erlangen, Germany, 6–9 April 2005

Bernini M, Vescovi P, Zanzucchi G (1997) Schema Strutturale dell'Appennino nord-occidentale. L'Ateneo Parmense-Acta Naturalia 33:43–54

Bertolini G, Pellegrini M (2001) The landslides of the Emilia Apennines (northern Italy) with reference to those which resumed activity in the 1994–1999 period and required Civil Protection interventions. Quad Geol Appl 8:27–74

Binaghi E, Luzi L, Madella P, Pergalani F, Rampini A (1998) Slope Instability Zonation: a comparison between Certainty Factor and Fuzzy Dempster–Shafer approaches. Nat Hazards 17:77–97

Boccia A (1804) Viaggio ai monti di Parma. Palatina, Parma

Bonham-Carter GF (1994) Geographic information systems for geoscientists: modelling with GIS. Computer Methods in the Geosciences 13, Pergamon

Brabb EE (1984) Innovative approaches to landslide hazard mapping. In: Proceedings of the IV international symposium on landslides, Toronto, vol. 1, pp 307–324

Brabb EE, Pampeyan EH, Bonilla MG (1972) Landslide susceptibility in San Mateo County, California. Misc Field Studies Map MF360 (scale 1:52,500). U.S. Geological Survey, Reston, Va

Çevik E, Topal T (2003) GIS-based landslide susceptibility mapping for a problematic segment of the natural gas pipeline, Hendek (Turkey). Environ Geol 44:949–962

Carrara A, Cardinali M, Detti R, Guzzetti F, Pasqui V, Reichenbach P (1991) GIS techniques and statistical models in evaluating landslide hazard. Earth Surf Process Landforms 16:427–445

Carrara A, Cardinali M, Guzzetti F (1992) Uncertainty in assessing landslide hazard and risk. ITC J 2:172–183

Carrara A, Cardinali M, Guzzetti F, Reichenbach P (1995a) GIS technology in mapping landslide hazard. In: Carrara A,Guzzetti F (eds) Geographical information systems in assessing natural hazards. Kluwer, Dordrecht, pp 135–175

Carrara A, Cardinali M, Guzzetti F, Reichenbach P (1995b) GIS-based techniques for mapping landslide hazard. (http://www.deis158.deis.unibo.it/gis/chapt0.htm)

Cerrina Feroni A,Vescovi P (2005) Foglio 217 "Neviano degli Arduini" della Nuova Carta Geologica d'Italia 1: 50.000. Servizio Geologico d'Italia, Roma

Cerrina Feroni A, Elter P, Plesi G, Rau A, Rio D, Vescovi P, Zanzucchi G (1990) Carta Geologica dell'Appennino emiliano-romagnolo 1:50.000. Foglio no 217 "Neviano degli Arduini". Selca, Firenze

Chung CF, Fabbri AG (1999) Probabilistic prediction models for landslide hazard mapping. Photogrammetric Eng Remote Sensing 65:1389–1399

Chung CF, Fabbri AG (2003) Validation of spatial prediction models for landslide hazard mapping. Nat Hazards 30:451–472

Chung CF, Fabbri AG, van Westen CJ (1995) Multivariate regression analysis for landslide hazard zonation. In: Carrara A, Guzzetti F (eds) Geographical information systems in assessing natural hazards. Kluwer, Dordrecht, pp 107–133

Chung CF, Kojma H, Fabbri AG (2002) Stability analysis of prediction models for landslide hazard mapping. In: Allison RJ (ed) Applied geomorphology: theory and practice, pp 3–19

Clerici A (2002) A GRASS GIS based shell script for landslide susceptibility zonation. In: Proceedings of the open source free software GIS-GRASS users conference. Trento, Italy 11–13 September 2002 (http://www.ing.unitn.it/~grass/conferences/GRASS2002/proceedings/proceedings/pdfs/Clerici_Aldo.pdf).

Clerici A, Cuccuru G, Trambaglio L, Lina F (1993) La realizzazione di una carta della stabilità dei versanti mediante l'uso di un Sistema d'Informazione Geografica. Geologia Tecnica Ambientale 4/93:25–40

Clerici A, Perego S, Tellini C, Vescovi P (2002) A procedure for landslide susceptibility zonation by the conditional analysis method. Geomorphology 48:349–364

Cooper M (2005) Advanced bash-scripting guide. An in-depth exploration of the art of shell scripting (Revision 3.6) (http://www.en.tldp.org/LDP/abs/html/)

Cruden DM, Hu XQ (1996) Hazardous modes of rock slope movement in the Canadian Rockies. Environ Eng Geosci 2:507–516

Cruden DM, Varnes DJ (1996) Landslide types and processes. In: Turner AK, Schuster RL (eds) Landslides: investigation and mitigation. Transportation research board special report 247, pp 36–75

Dai FC, Lee CF (2002) Landslide characteristics and slope instability modeling using GIS, Lantau Island, Hong Kong. Geomorphology 42:213–228

Dai FC, Lee CF (2003) A spatiotemporal probabilistic modeling of storm-induced shallow landsliding using aerial photographs and logistic regression. Earth Surf Process Landforms 28:527–545

Dai FC, Lee CF, Ngai YY (2002) Landslide risk assessment and menagement: an overview. Eng Geol 64:65–87

Dall'Olio E (1975) Itinerari turistici della Provincia di Parma. Artegrafica Silva, Parma

D'Amato Avanzi G, Giannecchini R, Puccinelli A (2004) The influence of the geological and geomorphological settings on shallow landslides. An example in a temperate climate environment: the June 19, 1996 event in northwestern Tuscany (Italy). Eng Geol 73:215–228

Di Dio G, Lasagna S, Preti D, Sagne M (1997) Carta Geologica dei depositi quaternari della Provincia di Parma. Il Quaternario 10:445–452

Donati L, Turrini MC (2002) An objective method to rank the importance of the factors predisposing to landslides with the GIS methodology: application to an area of the Apennines (Valnerina; Perugia, Italy). Eng Geol 63:277–289

Elter P, Grasso M, Parotto M, Vezzani L (2003) Structural setting of the Apennine-Maghrebian thrust belt. Episodes 26:205–211

Ercanoglu M, Gokceoglu C (2004) Use of fuzzy relations to produce landslide susceptibility map of a landslide prone area (West Black Sea Region, Turkey). Eng Geol 75:229–250

Ermini L, Catani F, Casagli N (2005) Artificial Neural Network applied to landslide susceptibility assessment. Geomorphology 66:327–343

Fernandes NF, Guimarães RF, Gomes RAT, Vieira BC, Montgomery DR, Greenberg H (2004) Topographic controls of landslides in Rio de Janeiro: field evidence and modelling. Catena 55:163–181

Fernandez T, Irigaray C, El Hamdouni R, Chacón J (2003) Methodology for Landslide Susceptibility Mapping by means of a GIS. Application to the Contraviesa Area (Granada, Spain). Nat Hazards 30:297–308

Free software foundation (2002) Bash reference manual (Edition 2.5b) (http://www.gnu.org/software/bash/manual/bashref.html)

Free Software Foundation (2003) The GNU Awk User's Guide (Edition 3)(http://www.gnu.org/software/gawk/manual/gawk.html)

GRASS Development Team (1999) GRASS: geographic resources analysis support system (http://www.grass.itc.it)
Guzzetti F, Carrara A, Cardinali M, Reichenbach P (1999) Landslide hazard evaluation: a review of current techniques and their application in a multi-scale study, Central Italy. Geomorphology 31:181–216
Jakob M (2000) The impacts of logging on landslide activity at Clayoquot Sound, British Columbia. Catena 38:279–300
Ko Ko C, Flentje P, Chowdhury R (2004) Landslides qualitative hazard and risk assessment method and its reliability. Bull Eng Geol Env 63:149–165
Lan HX, Zhou CH, Wang LJ, Zhang HY, Li RH (2004) Landslide hazard spatial analysis and prediction using GIS in the Xiaojiang watershed, Yunnan, China. Eng Geol 76:109–128
Larsen MC, Torres-Sánchez AJ (1998) The frequency and distribution of recent landslides in three montane tropical regions of Puerto Rico. Geomorphology 24:309–331
Lee S (2004) Application of likelihood ratio and logistic regression models to landslide susceptibility mapping using GIS. Environ Manage 34:223–232
Lee S, Choi J (2004) Landslide susceptibility mapping using GIS and the weight-of-evidence model. Int J Geogr Inf Sci 18:789–814
Lee S, Chwae U, Min K (2002) Landslide susceptibility mapping by correlation between topography and geological structure: the Janghung area, Korea. Geomorphology 46:149–162
Lee S, Choi J, Woo I (2004) The effect of spatial resolution on the accuracy of landslide susceptibility mapping: a case study in Boun, Korea. Geosci J 8:51–60
Lin ML, Tung CC (2003) A GIS-based potential analysis of the landslides induced by the Chi-Chi earthquake. Eng Geol 71:63–77
Lineback Gritzner M, Marcus WA, Aspinall R, Custer SG (2001) Assessing landslide potential using GIS, soil wetness modeling and topographic attributes, Payette River, Idaho. Geomorphology 37:149–165
Lopez HJ, Zink JA (1991) GIS-assisted modelling of soil-induced mass movement hazards: a case study of the upper Coello river basin, Tolima, Colombia. ITC J 4:202–220
Luzi L, Pergalani F (1999) Slope instability in static and dynamic conditions for urban planning: the 'Oltre Po Pavese' case history (Regione Lombardia-Italy). Nat Hazards 20:57–82
Menéndez Duarte R, Marqínez J (2002) The influence of environmental and lithologic factors on rockfall at a regional scale: evaluation using GIS. Geomorphology 43:117–136
Moreiras SM (2005) Landslide susceptibility zonation in the Rio Mendoza Valley, Argentina. Geomorphology 66:345–357
Nagarajan R, Roy A, Vinod Kumar R, Mukherjee A, Khire MV (2000) Landslide hazard susceptibility mapping based on terrain and climatic factors for tropical monsoon regions. Bull Eng Geol Env 58:275–287
Neteler M, Mitasova H (2004) Open source GIS: a GRASS GIS approach, 2nd edn. Kluwer, Dordrecht
Ohlmacher GC, Davis JC (2003) Using multiple logistic regression and GIS technology to predict landslide hazard in northeast Kansas, USA. Eng Geol 69:331–343
Perotto-Baldiviezo HL, Thurow TL, Smith CT, Fisher RF, Wu XB (2004) GIS-based spatial analysis and modeling for landslide hazard assessment in steeplands, southern Honduras. Agric Ecosys Environ 103:165–176
Pinna M, Vittorini S (1985) Contributo alla determinazione dei regimi pluviometrici in Italia. In: Contributi di climatologia. Mem Soc Geogr It 39:147–167
Pizzini K (1998) sed, a stream editor (version 3.02). Free Software Foundation, Boston, MA (http://www.gnu.org/software/sed/manual/html_chapter/sed_-toc.html)
Raghavan V, Masumoto S, Kajiyama A, Nemoto T, Fujita T (2004) Landslide hazard zonation using the GRASS GIS: a case study in the Ojiya District, Niigata Prefecture, Japan Int Symposium on Geoinformatics for Spatial Infrastructure Development in Earth and Allied Sciences. Hanoi, Vietnam, September 16–18, 2004 (http://www.gisws.media.osaka-cu.ac.jp/gisideas04/viewpaper.php?id = 88)
Remondo J, Gonzales A, Díaz De Terán JR, Cendrero A, Fabbri A, Chung CF (2003) Validation of landslide susceptibility maps; examples and applications from a case study in Northern Spain. Nat Hazards 30:437–449
Santacana N, Corominas J (2002) Example of validation of landslide susceptibility maps. In: Rybář J, Stemberk J, Wagner P (eds) Landslides. Sweets& Zetlinger, Lisse, pp 305–310
Santacana N, Baeza B, Corominas J, De Paz A, Marturiá J (2003) A GIS-based multivariate statistical analysis for shallow landslide susceptibility mapping in La Pobla de Lillet Area (Eastern Pyrenees, Spain). Nat Hazards 30:281–295
Shrestha DP, Zink JA, Van Ranst E (2004) Modelling land degradation in the Nepalese Himalaya. Catena 57:135–156
Soeters R, van Westen CJ (1996) Slope instability recognition, analysis, and zonation. In: Turner AK, Schuster RL (eds) Landslides: investigation and mitigation. Transportation Research Board Special Report 247, pp 129–177
Süzen ML, Doyuran V (2004) Data driven bivariate landslide susceptibility assessment using geographical information systems: a method and application to Asarsuyu catchment, Turkey. Eng Geol 71:303–321
Tangestani MH (2004) Landslide susceptibility mapping using the fuzzy gamma approach in a GIS, Kakan catchment area, southwest Iran. Aust J Earth Sci 51:439–450
Tellini C, Chelli A (2003) Ancient and recent landslide occurrences in the Emilia Apennines (Northern Apennines, Italy). In: Proceedings of the workshop on geomorphological sensitivity and system response, Camerino-Modena Apennines (Italy), July 4–9 2003, pp 105–114
Vescovi P (1998) Le Unità Subliguri dell'alta Val Parma (Provincia di Parma). Atti Tic Sc Terra 40:215–231
Vescovi P (2002) Foglio 216 "Borgo Val di Taro" della Nuova Carta Geologica d'Italia 1:50.000. Servizio Geologico d'Italia, Roma
Vescovi P, Fornaciari E, Rio D, Valloni R (1999) The basal complex stratigraphy of the Helminthoid Monte Cassio Flysch: a key to Eoalpine tectonics of the Northern Apennines. Rivista Italiana di Paleontologia e Stratigrafia 105:101–128
van Westen CJ, Rengers N, Soeters R (2003) Use of geomorphological information in indirect landslide susceptibility assessment. Nat Hazards 30:399–419
Zêzere JL, Ferreira AB, Rodrigues ML (1999) The role of conditioning and triggering factors in the occurrence of landslides: a case study in the area north of Lisbon (Portugal). Geomorphology 30:133–146
Zhou CH, Lee CF, Li J, Xu ZW (2002) On the spatial relationship between landslides and causative factors on Lantau Island, Hong Kong. Geomorphology 43:197–207